Journal of Engineering Physics and Thermophysics, Vol. 80, No. 6, 2007

NUMERICAL SIMULATION OF CRISIS PHENOMENA IN A SUBSONIC AIR FLOW AROUND A THICK AIRFOIL WITH VORTEX CELLS

S. A. Isaev,[a] A. G. Sudakov,[b] P. A. Baranov,[a] and N. A. Mordynskii[a]

UDC 532.517.4

Crisis phenomena arising in a subsonic air flow around a thick airfoil with vortex cells have been numerically simulated in the process of solving the nonstationary equations of mass and energy conservation and Reynolds equations closed by a model of shear-stress transfer with the use of the finite-volume factorization method.

Introduction. The design of an ÉKIP ("Ékologiya I Progress") flying vehicle shaped as a small-aspect-ratio thick airfoil resembling a flying plate, proposed in [1] (Fig. 1a), initiated numerical investigations on the development of methods for control of flows around bodies, in particular, a circular cylinder, with the use of vortex cells built into their profile [2, 3]. Within the framework of the generalized conception [4], cavities, trenches, holes, and clearances between bodies of different dimension, including those with central bodies built into them, are considered as vortex cells. In this conception, both passive and active vortex cells are used. It is assumed that a flow circulating in an active vortex cell is subjected to an energy action (produced by a suction, a movement of a part of the cell profile around which a stream flows, or a rotation of a central body).

The configuration of a vortex cell (Fig. 1b) is topologically formalized by an elliptic profile with a central body built into it. The central body serves for intensification of the flow circulating in the cell; in this case, the well-known method of suction distributed over the surface of a body or, when a body is cylindrical, the method of twisting of the flow around it with a constant angular velocity is used. In the case where a central body is absent, the flow in a cell is intensified by a lumped (discontinuously distributed) suction or, theoretically, by the movement of a portion of its profile. As a varied local parameter acting on the flow circulating in the cell, the rate of suction or the tangential velocity of the flow at the moving wall is selected, and, as an integral factor, the volumetric dimensionless rate of flow C_q expressed in terms of the characteristic velocity and length scales is used.

Several vortex cells can be built into an object. The dimensions of the cells are selected empirically; they comprise small fractions of the characteristic dimensions of the body. In addition to the geometrical parameters of a vortex cell, the dimensions of a window, the coordinates of its center on the profile of the body, and the radii of the roundings of the transition parts between the profile of the cell and the generatrix of the body are considered (Fig. 1b). In this way, a streamlined surface of the body with curvilinear slots–vortex cells is formed; it is appropriate to locate these cells in the neighborhood of the flow separations on the profile of the body. Vortex cells are introduced for the purpose of organization of a near-nonseparation flow around the body and, therefore, for improvement of its aerodynamic characteristics.

In [5–17], methods of control of laminar and turbulent flows of an incompressible fluid around large-aspect-ratio ÉKIP airfoils equipped with a system of active vortex cells were considered. In these works, the operating parameters of the vortex cells, providing a flow without separation around a thick airfoil, an additional circulation (the supercirculation effect), and an increase in the aerodynamic lift, have been determined. The large lift coefficient $C_y > 1$ was obtained in the wide range of angles of attack from -30^o to $+25^o$. The superiority, in aerodynamic characteristic, of thick profiles with vortex cells over thin profiles, including those equipped with units of control of a flow around them, was demonstrated.

[a]St. Petersburg State University of Civil Aviation, 38 Pilotov Str., St. Petersburg, 196210, Russia; [b]Rigel' Accumulation Company, 38 Popov Str., St. Petersburg, 197376, Russia. Translated from Inzhenerno-Fizicheskii Zhurnal, Vol. 80, No. 6, pp. 122–126, November–December, 2007. Original article submitted April 18, 2007.

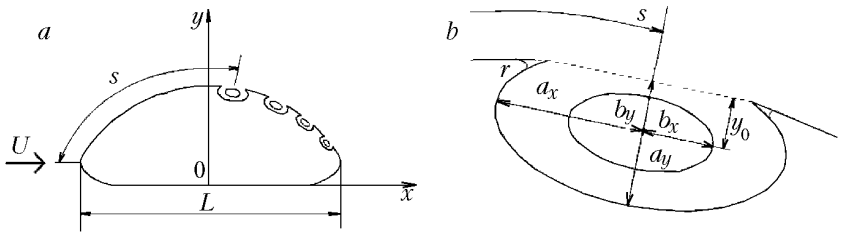

Fig. 1. ÉKIP airfoil of thickness 0.373 with vortex cells (a) and an elliptically shaped vortex cell with rounded pointed edges (b).

The aim of the present work is to investigate the influence of the compressibility of a fluid on the flow of this fluid around an ÉKIP airfoil with vortex cells (Fig. 1a). As in [11–15], we considered an airfoil with slightly rounded leading and trailing edges, and the rate of suction of fluid from the surface of the central-bodies located in the cells was assumed to be equal to 0.05 of the characteristic velocity of the incident flow U. The quantities being considered were brought to the dimensionless form and expressed in terms of the flow density and the airfoil-chord length L. The angle of attack was assumed to be equal to zero. The intensity of the flows circuiting in the cells was very high and, consequently, the compressibility of the fluid significantly influenced the flow around the airfoil even at moderate Mach numbers.

The profile of a streamlined body is formed by an upper circular arc with a radius of 0.577 and two lower circular arcs of radius 0.175, connected by a straight line with a coordinate $y = -0.0866$. The radius of the rounding of the leading and trailing edges is equal to 0.05. The arc coordinate of the center of the first-cell window is 0.685, and the length of this window is 0.0834. The elliptic-shape cells (Fig. 1b) with longitudinal and transverse semi-axes $a_x = 0.0584$ and $a_y = 0.5a_x$ are built into the thick profile at a depth $y_0 = 0.7a_y$. At the centers of the cells, elliptically shaped central bodies with semi-axes of $0.5a_x$ and $0.25a_x$ are located. The other three cells with arc coordinates 0.861, 0.992, and 1.107 are topologically identical to the first cell and have windows of size 0.0696, 0.0556, and 0.0417. The longitudinal semiaxes of the elliptical cells are 0.0487, 0.0389, and 0.0292, and the radii of the roundings of their edges are 0.00084, 0.00067, and 0.00051.

Formulation of the Problem and Method of Solution. A stationary, uniform, two-dimensional motion of air in a cylindrical computational region is considered. The center of this region is coincident with the origin of the Cartesian coordinate system x, y (Fig. 1a). The outer boundary of the computational region is at a large distance (38.62 chords) from a body. The parameters of the flow at the input part of the boundary of this region are fixed, and soft boundary conditions (the conditions of solution continuation) are set at its output part. The parameters of turbulence at the input to the computational region are identical to those in the problem on an incompressible-viscous flow [5–17]: the degree of turbulence of the external flow is at the level characteristic of a wind tunnel, $\mathrm{Tu}_\infty = 1.5\%$, and the scale of turbulence is assumed to be equal to the airfoil chord. On the thermally insulated surfaces, around which a stream flows, the adhesion conditions are fulfilled. In the incident flow, the Reynolds number Re_∞, equal to 10^5, remains unchanged (at this value of Re_∞ the aerodynamic characteristics of the medium are practically independent of its viscosity) and the Mach number M_∞ varies from 0 to 0.5. The Prandtl number for air is 0.7 and the turbulent Prandtl number is assumed to be equal to 0.9.

The airfoil is surrounded by a three-stage computational grid. The annular layer of thickness 0.13, adjacent to the airfoil profile, contains 51 nodes in the transverse direction. Within the distance from the airfoil-profile nose to the first vortex cell, 121 nodes are located, 16 nodes are in the cells, 26 nodes are between the cells, and 201 nodes are located within the distance from the last cell to the leading edge of the airfoil profile. The grid pitch near the surface is equal to 0.0005. The second and third annular layers of thickness 3 and 35 contain 101 and 41 nodes in the radial direction and 421 nodes along the circumferential coordinate.

Each vortex cell is covered by an individual external grid adjacent to its window. The vertical sizes of all the subregions are 0.1, the number of nodes along the normal to the wall is 51, and the near-wall pitch is 0.001. The computational nodes bunch in the neighborhood of the edges. The near-edge pitch is assumed to be equal to 0.001. Within each vortex cell, a cylindrical grid with a bunching of nodes near the walls of the cell, the central body (the

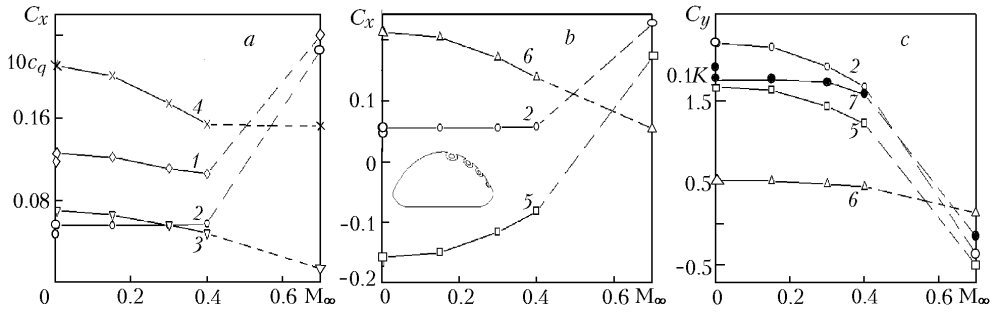

Fig. 2. Dependence of the drag (a) and lift (c) coefficients and their components (b, c) determined for the ÉKIP airfoil, the scaled values of the lift-drag ratio (c), and the flow coefficient (a) on M_∞: 1) $C_{x\text{int}}$; 2) C_x, C_y; 3) $C_{x\text{add}}$; 4) $10c_q$; 5) $C_{x\text{pr}}$, $C_{y\text{pr}}$; 6) $C_{x\text{cell}}$, $C_{y\text{cell}}$; 7) 0.1 K.

near-wall pitch is 0.0001), and the pointed edges (a minimum pitch is 0.001) is constructed. The zones of the leading and trailing edges of the vortex cells are covered by curvilinear fine grids, much as was done in [14, 17].

By analogy with the approach used in [8–17], the additional drag $C_{x\text{add}}$ of the airfoil with vortex cells is determined, in the case of suction from the surface of the central body, by the energy necessary for the maintenance of the flow rate of the sucked air. As a result, the drag coefficient of the cylinder with vortex cells, corrected for the expenditure of energy, is determined as $C_{x\text{int}} = C_x + C_{x\text{add}}$; this coefficient is used for determining the lift-drag ratio $K = C_y/C_{x\text{int}}$.

A turbulent flow of a compressible viscous gas around the ÉKIP airfoil with vortex cells is calculated using a modified VP2/3 package, in which the multiblock computational technologies developed in [13, 16, 17] are used for solving the stationary equations of mass and energy conservation and the Reynolds equations closed by the equations of shear-stress transfer [18]. The SIMPLEC procedure of pressure correction is generalized for the case of compressible turbulent flows, including those with compression shocks. As follows from [19, 20], to stabilize the computational process, it makes sense to approximate the convective terms of the Reynolds equations by the Lenard scheme and the convective terms of the other equations by the Van Leer scheme [17].

Discussion of the Results. Figures 2 and 3 present some of the results of investigation of the influence of the number M_∞ on the aerodynamic characteristics and the pattern of flow around the ÉKIP airfoil being considered.

It should be noted that, at a definite volumetric rate of the sucked-air flow $C_q = 0.0212$, the mass flow c_q decreases with increase in M_∞ (Fig. 2a, curve 4). As a consequence, at small values of M_∞, the additional drag of the profile, which is due to the expenditure of energy $C_{x\text{add}}$, decreases (curve 3). However, the calculated drag coefficient C_x (curve 2) remains practically unchanged in the range of $M_\infty = 0$–0.4, which causes a fairly moderate decrease in the total drag of the thick ÉKIP airfoil $C_{x\text{int}}$ (curve 1).

In the range of change in M_∞ from 0.4 to 0.7, we failed to obtain a stationary solution of the problem; therefore, the dependences of the integral characteristics on M_∞ are denoted by the dashed lines in Fig. 2. It may be suggested that a flow around the airfoil being considered is nonstationary and cyclic in character. However, at $M_\infty = 0.7$ the results obtained differ markedly from the results obtained for small M_∞. In this case, the total drag is more than two times larger and reaches 0.24, and $C_{x\text{add}}$ decreases sharply (by a factor of seven as compared to that at $M_\infty = 0$). It is interesting that c_q remains at its value attained at $M_\infty = 0.4$.

The calculated drag of the airfoil C_x, as follows from Fig. 2b, consists of two components: the drag of the airfoil itself $C_{x\text{pr}}$ (curve 5) and the total drag of the vortex cells $C_{x\text{cell}}$ (curve 6). As may be seen, at small values of M_∞, the airfoil is acted upon by a driving force since $C_{x\text{pr}} < 0$, and all of the drag force is concentrated in the profiles of the vortex cells. When M_∞ increases, there appear tendencies for an increase in $C_{x\text{pr}}$ and a decrease in $C_{x\text{cell}}$. At values of M_∞ smaller than 0.4, these tendencies completely compensate each other, while at $M_\infty = 0.7$, both components of C_x are positive and the drag of the airfoil itself prevails over the drag of the vortex cells.

As follows from Fig. 2c, the lift coefficient C_y of the airfoil with vortex cells is maximum at $M_\infty = 0$. When M_∞ increases, the coefficient C_y and its components decrease monotonically, and, at small values of M_∞, $C_{y\text{pr}}$ (curve

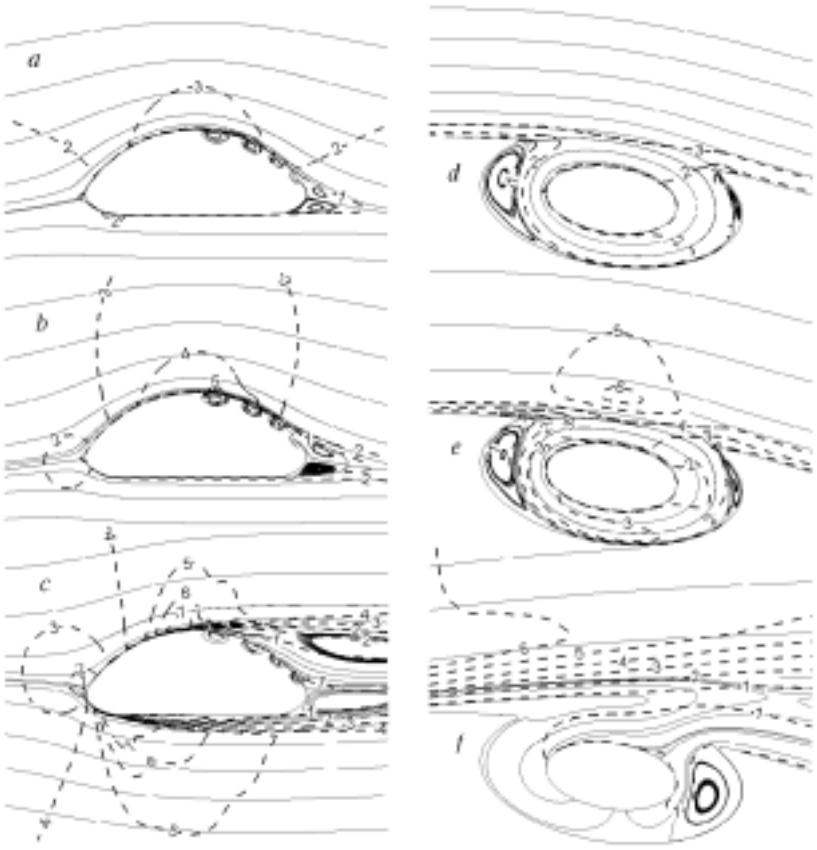

Fig. 3. Comparative analysis of the patterns of flow around the ÉKIP airfoil with vortex cells (a–c) and the patterns of flow in the neighborhood of the first vortex cell (d–f) with isomaches (denoted by the dashed lines) determined for different values of M_∞: M_∞ = 0.3 (a, d); 0.4 (b, e), and 0.5 (c, f); 1–7) M = 0.1, 0.3, 0.5, 0.7, 0.9, 1, 1.1.

5) exceeds $C_{y\text{cell}}$ (curve 6). At M_∞ = 0.7, the ÉKIP airfoil with vortex cell has no aerodynamic lift, i.e., $C_y < 0$. However, $C_{y\text{cell}}$ remains positive, even though its value is small.

And, lastly, the lift-drag ratio of the airfoil with vortex cells (curve 7) remains stable and large (K = 18) at small values of M_∞ until M_∞ = 0.3 because the rates of decrease in C_y and $C_{x\text{int}}$ with increase in M_∞ are equal. However, $K < 0$ at M_∞ = 0.7.

The evolution of the pattern of flow around the ÉKIP profile with increase in M_∞ explains the behavior of its aerodynamic characteristics to a large extent (Fig. 3). The increase in the dimensions of the separation zone in the near wake downstream of the airfoil correlates with the decrease in the total drag (Fig. 3a and b), and, even at M_∞ = 0.4, in the neighborhood of the first vortex cell (Fig. 3e), there arises a local supersonic zone. It should be noted that the pattern of a separation flow in a vortex cell changes insignificantly with increase in M_∞ from 0.3 to 0.4 (Fig. 3d and e). The change to M_∞ = 0.7 causes a transformation of the pattern of flow around the thick airfoil (Fig. 3c) with a flow separation upstream of the system of vortex cells, and the cells find themselves within the separation zone in the near wake. The structure of the separation flow in the cells also changes substantially (Fig. 3f).

Conclusions. It has been established that there exist critical Mach numbers of the incident flow M_∞ at which there arise crisis phenomena and the system of control of the flow around a thick airfoil with vortex cells becomes ineffective. These numbers fall within the range 0.4–0.5 at a moderate (0.025) flow rate C_q.

This work was carried out with financial support from the Russian Foundation for Basic Research (project Nos. 06-08-81002 and 05-01-00162) and the European Union in accordance with the Framework-6 Program (project VortexCell2050).

NOTATION

a_x, a_y, sizes of the semi-axes of an elliptical vortex cell, fractions of L; b_x, b_y, sizes of the semi-axes of an elliptical central body, fractions of L; C_x, drag coefficient; $C_{x\text{add}}$, coefficient of the additional drag that is due to the expenditure of energy for the maintenance of suction from the surface of the central bodies; $C_{x\text{int}}$, drag coefficient corrected with account for the expenditure of energy; C_y, lift coefficient; C_q, rate of flow through the surface of the central body, fractions of UL; c_q, rate of flow through the surface of the central body, fractions of ρUL; K, lift-drag ratio ($K = C_y/C_{x\text{int}}$); L, chord length, m; Re, Reynolds number ($\text{Re} = \rho UL/\mu$); r, radius of a rounding, fractions of L; s, dimensionless coordinate along the profile of the cylinder expressed in terms of the chord; Tu, degree of turbulence of the flow, fractions of U; U, velocity of an undisturbed flow, m/sec; x, y, dimensionless Cartesian coordinates in the coupled systems expressed in terms of the chord; y_0, coordinates of the center of a cell, fractions of L; μ, dynamic viscosity coefficient, kg/(m·sec); ρ, density of a fluid, kg/m^3. Subscripts: add, additional; cell, loads on only the vortex cells; int, summarized; pr, loads on the airfoil itself; ∞, parameter of an undisturbed flow.

REFERENCES

1. L. N. Shchukin, Flying vehicles "ÉKIP," *Grazhd. Aviatsiya*, No. 6, 11–15 (1993).
2. P. A. Baranov, S. A. Isaev, Yu. S. Prigorodov, and A. G. Sudakov, Numerical simulation of a laminar flow around a cylinder with passive and active vortex cells within the framework of the concept of decomposition of a computational region and with the use of multistage grids, *Pis'ma Zh. Tekh. Fiz.*, **24**, Issue 8, 33–41 (1998).
3. P. A. Baranov, S. A. Isaev, Yu. S. Prigorodov, and A. G. Sudakov, Numerical simulation of the effect of decrease in the drag of a cylinder with vortex cells equipped with a system for control of a turbulent boundary layer, *Pis'ma Zh. Tekh. Fiz.*, **24**, Issue 17, 16–23 (1998).
4. S. A. Isaev and A. I. Leont'ev, The concept of a generalized vortex cell and its use in the aerodynamics of thick profiles and technologies of holes, in: *Abstracts of the papers submitted to the 9th All-Union Congress on Theoretical and Applied Mechanics*, Vol. 2, NNGU, Nizhnii Novgorod (2006), pp. 96–97.
5. P. A. Baranov, S. A. Isaev, Yu. S. Prigorodov, and A. G. Sudakov, Calculation of a laminar flow around a profile with passive and active vortex cells on multiblock intersecting grids, *Izv. Vys. Uchebn. Zaved., Aviats. Tekh.*, No. 3, 30–35 (1999).
6. P. A. Baranov, S. A. Isaev, Yu. S. Prigorodov, and A. G. Sudakov, Numerical simulation of the effect of increase in the lift-drag ratio of profiles due to the suction in vortex cells, *Inzh.-Fiz. Zh.*, **72**, No. 3, 572–575 (1999).
7. P. A. Baranov, S. A. Isaev, Yu. S. Prigorodov, and A. G. Sudakov, Numerical analysis of the influence of the angle of attack on a turbulent incompressible-fluid flow past a thick profile with vortex cells, *Inzh.-Fiz. Zh.*, **73**, No. 4, 719–727 (2000).
8. S. A. Isaev, A. G. Sudakov, P. A. Baranov, and Yu. S. Prigorodov, Effect of supercirculation in a flow around a thick profile with vortex cells, *Dokl. Ross. Akad. Nauk*, **377**, No. 2, 198–200 (2001).
9. S. A. Isaev, Yu. S. Prigorodov, and A. G. Sudakov, Analysis of the efficiency of control of flows about bodies with the use of vortex cells with allowance for the expenditure of energy, *Inzh.-Fiz. Zh.*, **75**, No. 3, 47–50 (2002).
10. S. A. Isaev, Yu. S. Prigorodov, A. G. Sudakov, and D. P. Frolov, Numerical simulation of the influence of the viscosity on a turbulent flow around a thick airfoil with vortex cells, *Inzh.-Fiz. Zh.*, **75**, No. 6, 100–103 (2002).
11. S. A. Isaev, P. A. Baranov, N. A. Kudryavtsev, I. A. Pyshnyi, and V. B. Kharchenko, Numerical simulation of a nonstationary turbulent flow around a thick profile with vortex cells in the presence of a suction from the surface of the central bodies, *Aéromekh. Gaz. Dinam.*, No. 3, 3–15 (2002).
12. S. A. Isaev, I. A. Pyshnyi, A. Yu. Snegirev, A. E. Usachov, and V. B. Kharchenko, Multiblock computational technologies of solving fundamental, applied, and operational problems of power engineering and transport, in:

G. A. Kryzhanovskii and E. A. Kuklev (Eds.), *Scientific Bulletin of the Academy of Civil Aviation. Series: Problems in Flight Safety and Maintenance of Air Transport*, No. 1, 50–58 (2003).

13. A. V. Ermishin and S. A. Isaev (Eds.), *Control of Flows around Bodies with Vortex Cells as Applied to Flying Vehicles of Integral Arrangement* (*Numerical and Physical Simulation*) [in Russian], MGU, Moscow (2003).
14. P. A. Baranov, S. A. Isaev, Yu. S. Prigorodov, and A. G. Sudakov, Control of a turbulent flow around a thick profile in the case of intensification of the flow in the vortex cells due to the suction from the surface of central bodies, *Izv. Ross. Akad. Nauk*, *Mekh. Zhidk. Gaza*, No. 3, 57–68 (2003).
15. S. A. Isaev, P. A. Baranov, N. A. Kudryavtsev, I. A. Pyshnyi, and A. G. Sudakov, Numerical analysis of the influence of the angle of attack on a turbulent flow around a thick profile with vortex cells at high Reynolds numbers, *Inzh.-Fiz. Zh.*, **76**, No. 4, 115–124 (2003).
16. S. A. Isaev, P. A. Baranov, N. A. Kudryavtsev, D. A. Lysenko, and A. E. Usachov, Multiblock computational technologies for solving problems of hydraulics and aeromechanics, *Nauch.-Tekh. Vedom. SPbGPU*, No. 1(39), 48–59 (2005).
17. Yu. A. Bystrov, S. A. Isaev, N. A. Kudryavtsev, and A. I. Leont'ev, *Numerical Simulation of a Vortex Intensification of Heat Transfer in Bunches of Pipes* [in Russian], Sudostroenie, St. Petersburg (2005).
18. F. R. Menter, Zonal two-equation k-ω turbulence models for aerodynamic flows, *AIAA Paper*, No. 93–2906 (1993).
19. P. A. Baranov, S. A. Isaev, A. N. Mikhalev, and A. G. Sudakov, Calculation of sub-, super-, and hypersonic flows around a drop-like cupped body with the use of the model of shear-stress transfer, in: *Proc. Int. Conf. "Problems of Ballistics-2006"* and of the *5th Int. School-Seminar "Intrachamber Processes*, *Combustion*, *and Gas Dynamics of Disperse Systems* [in Russian], Vol. 2, St. Petersburg (2006), pp. 40–43.
20. P. A. Baranov, S. A. Isaev, A. I. Leont'ev, and A. E. Usachov, Numerical simulation of a decrease in the aerodynamic heating of a profile with spherical and honeycomb holes at super- and hypersonic velocities, in: *Proc. 4th Russian National Conf. on Heat Transfer*, Vol. 6, *Disperse Flows and Porous Media. Enhancement of Heat Transfer* [in Russian], Izd. Dom MEI, Moscow (2006), pp. 158–161.